Desertification Information Extraction Along the China–Mongolia Railway Supported by Multisource Feature Space and Geographical Zoning Modeling

Haishuo Wei, Juanle Wang, and Baomin Han

***Abstract*—The China–Mongolia railway is the core foundation for the construction of traffic connection in the China–Mongolia–Russia economic corridor. Long-term desertification has brought significant ecological risks to the railway area. Owing to the large variety of vegetation cover in this region, desertification information is easily confused with other weak vegetation cover information. This article proposes a refined desertification information extraction method based on multisource feature spaces and geographical zoning modeling. First, based on the geographical zoning, land cover, and vegetation coverage data for Mongolia, the railway area is divided into the Central provinces and their northern region, the Eastern Mongolian Plateau, and the Southern Gobi region. According to the vegetation coverage characteristics and the applicability of various feature space models to different geographical regions, Albedo–normalized difference vegetation index, Albedo–modified soil adjusted vegetation index, and Albedo–topsoil grain size index feature space models were constructed for three geographical regions. Faced with new challenges presented by global warming and the impact of monsoons on the classification and extraction of desertification information, we established a desertification classification system with six levels (severe desertification, high desertification, medium desertification, low desertification, withered grassland, and nondesertification) and complete desertification information extraction. The results show that the overall classification accuracy of the method selected in this article is 85.21%. We further analyzed the mechanism of this method, compared it with previous studies, and thereby proved that this method is feasible to extract the fine information of desertification in large areas and complex geographical environments.**

***Index Terms*—Monitoring, remote sensing.**

I. Introduction

THE China–Mongolia railway, which connects China and Mongolia, is the main cross-border transportation trunk line in the China–Mongolia–Russia region, and it is the core foundation of transportation connectivity for the construction of the China–Mongolia–Russia economic corridor in the Belt and Road Initiative. The China–Mongolia–Russia economic corridor is characterized by complex geography, fragile ecology, and serious desertification. Mongolia is the hotspot of global desertification [1]. In 2017, data from the Ministry of Natural Environment and Tourism of Mongolia showed that 76.8% of the land in the country had been desertified to varying degrees, and this trend is still spreading at a faster rate [2]. The increasingly serious desertification problem along the China–Mongolia railway (Mongolian section), along with the environmental changes poses a risk to the construction of transportation infrastructure and the region's sustainable development. Therefore, it is necessary to establish a refined desertification information extraction method to accurately assess the desertification conditions along the China–Mongolia railway.

The China–Mongolia railway is located in arid and semiarid areas, and its desertification information can be easily confused with other weak vegetation cover information. It is difficult to effectively extract desertification information in this region [3]. This is because of the sparse precipitation and intense evaporation, which results in scarce vegetation growth and simple vegetation group structures. Spectral lines often do not have typical healthy vegetation characteristics, and there are no obvious strong absorption valleys and reflection peaks, which makes the spectral information for vegetation obtained from remote sensing images extremely weak and even difficult to detect [4]. Although vegetation indexes have been widely used to depict land degradation because of its simplicity in the early stage [5]–[7], the vegetation coverage in arid and semiarid areas is relatively low, which causes the soil spectrum to interfere with vegetation indexes [8], [9]. Therefore, the application of

Manuscript received September 22, 2019; revised December 3, 2019; accepted December 20, 2019. Date of publication January 20, 2020; date of current version February 12, 2020. This work was supported in part by the National Nature Science Foundation of China under Grant 41971385, in part by the Strategic Priority Research Program (Class A) of the Chinese Academy of Sciences under Grants XDA19040501 and XDA2003020302, in part by the fund program of the Asia Research Center, Mongolia and Korea Foundation for Advanced Studies under Grant P2018-3606, and in part by the Construction Project of the China Knowledge Center for Engineering Sciences and Technology under Grant CKCEST-2019-3-6. *(Corresponding author: Juanle Wang.)*

H. Wei is with the School of Civil and Architectural Engineering, Shandong University of Technology, Zibo 255049, China, and also with the State Key Laboratory of Resources and Environmental Information System, Institute of Geographic Sciences and Natural Resources Research, Chinese Academy of Sciences, Beijing 100101, China (e-mail: weihs@lreis.ac.cn).

J. Wang is with the State Key Laboratory of Resources and Environmental Information System, Institute of Geographic Sciences and Natural Resources Research, Chinese Academy of Sciences, Beijing 100101, China, and also with the Jiangsu Center for Collaborative Innovation in Geographical Information Resource Development and Application, Nanjing 210023, China (e-mail: wangjl@igsnrr.ac.cn).

B. Han is with the School of Civil and Architectural Engineering, Shandong University of Technology, Zibo 255049, China (e-mail: hanbm@sdut.edu.cn).

Digital Object Identifier 10.1109/JSTARS.2019.2962830

a single remote vegetation information sensing method in arid and semiarid areas is often not ideal [10].

The use of remote sensing satellites to monitor desertification began in the 1970s [11]. Remote sensing data and index products have become more abundant since the 1990s [12]. At this stage, many large-scale desertification monitoring studies have emerged, using long time-series characteristics to reflect the Mongolian Plateau and surrounding areas. Liu *et al*. obtained fractional vegetation cover (FVC), modified soil adjusted vegetation index (MSAVI), Albedo, land surface temperature (LST), and temperature vegetation dryness index through the inversion of National Oceanic and Atmospheric Administration data and moderate-resolution imaging spectroradiometer (MODIS) data and then obtained desertification distribution data for China and Central Asia from 1995 to 2001 with a spatial resolution of 1 km [13]. Unurbaatar *et al*. used MODIS to extract the spatial distribution pattern of desertification for the Mongolian Plateau from 2001 to 2010 with a spatial resolution of 1 km and then analyzed its change trend [14]. Zhuo obtained normalized difference vegetation index (NDVI), MSAVI, FVC, LST, and drought index through the inversion of MODIS data, established a monitoring index system for desertification in the Mongolian Plateau, and then obtained a desertification status map of the Mongolian Plateau for 2006 with a spatial resolution of 1 km [15]. These studies generally rely on the long-time-series characteristics of satellite data and use one or more indexes to form large-scale data products with coarse resolution. However, these macroinformations are insufficient to reveal the status of desertification in detail and to provide accurate data to support the control of desertification and regional risk.

Since the beginning of the 21st century, some scholars have begun using multidimensional remote sensing information to construct models for desertification information extraction [16]–[18]. Zeng *et al*. used the feature space of Albedo–NDVI to reflect the surface cover, hydrothermal combination, and their changes in desertification areas [19]. They found that with the exacerbation of desertification, surface vegetation suffered serious damage, and the NDVI value decreased. At the same time, with the decrease in surface vegetation coverage, surface moisture decrease, and the value of Albedo increases accordingly. This means that multidimensional remote sensing data have clear biophysical significance. However, it cannot adequately express the vegetation conditions in sparse vegetation areas because of the influence of soil background on NDVI. An increasing number of studies have tried to use different types of vegetation indexes to extract desertification information. Qi *et al*. found that MSAVI could better eliminate or reduce the influence of soil and vegetation canopy background [20]. Feng *et al*. constructed an Albedo–MSAVI feature space model based on Landsat 8 data with a resolution of 30 m and applied it to the study of soil salinization [21]. Different degrees of desertification produce different topsoil textures, the more serious the desertification, the rougher the topsoil particle composition [22]. Therefore, topsoil grain size index (TGSI) can be used to represent the size of soil surface particles and as an evaluation index for desertification [23]. Munkhnasan *et al*. took NDVI, TGSI, and Albedo as the representative indexes of vegetation biomass, landscape pattern, and micrometeorology, respectively, to obtain a 30-m resolution map of desertification and completed the dynamic analysis of desertification in Hogno Khaan nature reserve, Mongolia [24]. In 2017, through experiments, Munkhnasan *et al*. found that NDVI was weakly correlated with TGSI, whereas NDVI was strongly correlated with Albedo, and TGSI was strongly correlated with Albedo [25]. This provided a basis for constructing the Albedo–TGSI feature space model. Based on Landsat 8 remote sensing images data, Wei *et al*. constructed three feature space models, including Albedo–NDVI, Albedo–MSAVI, and Albedo–TGSI, and analyzed their respective characteristics and applicable conditions in the northwest of Mongolia [3]. The above-mentioned studies reflect the advantages of multisource feature space modeling in revealing fine desertification information, but only local scale inversion results can be obtained, and the inversion ability to extend to larger geographical areas is lacking. The main reason for this is that the geographical differentiation characteristics of the study area were not combined with the applicability of the model. In addition, the applicability of the model was not clearly defined.

Aiming at the fine desertification extraction problem along the China–Mongolia railway, our article proposes a desertification information extraction model based on the multisource feature space and geographical partition. First, we seek the adaptability of the model to different geographical areas, such as vegetation and land cover, along the China–Mongolia railway. Then, we establish the regional desertification inversion model and obtain the desertification data products with a resolution of 30 m. This article would provide a refined inversion method and data product support for ecological risk control of desertification in this region.

II. Materials and Methods

A. Study Area

The China–Mongolia railway runs from Beijing to Ulaanbaatar and extends to Ulan-Ude station on the Siberian railway in Russia. It stretches from south to north within Mongolian territory and passes through the following major cities: Zamyn Uud (a frontier port between China and Mongolia), Sainshand (the fourth largest city in Mongolia), Bor Undur (a world-class fluorite production area) [26], Ulaanbaatar (Mongolia's capital and the largest city in Mongolia), Zonhala and Darhan (emerging industrial cities), Erdenet (the center of copper and molybdenum industries), and Suhbaatar (a frontier port between Mongolia and Russia).

In this article, the selected study area is within 200 km of the China–Mongolia railway (Mongolian section) on both sides (as shown in Fig. 1). It includes 15 provinces: Hovsgol, Arhangay, Bulgan, Orhon, Selenge, Darhan, Tov, Ulaanbaatar, Hentiy, Ovorhangay, Dundgovi, Govisumber, Suhbaatar, Dornogovi, and Omnogovi. The overall topography of the study area is flat plateau with vast grassland distribution. It has temperate continental climate, with obvious seasonal changes. Spring and autumn are short, and the precipitation is low, with 70% of the precipitation concentrated in July and August. Strong winds and rapid weather changes are obvious characteristics of this region.

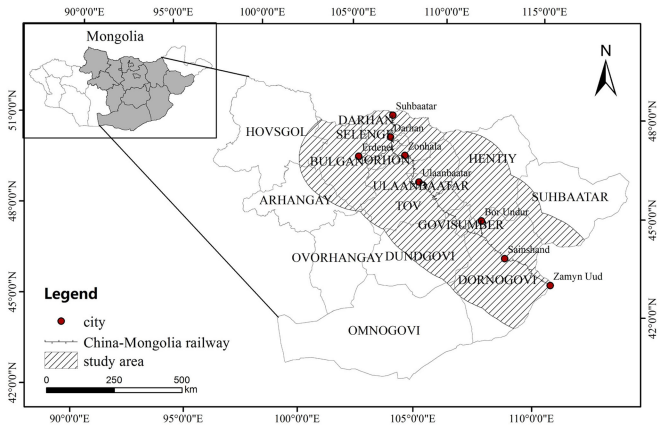

Fig. 1. Geographic location of the study area.

The main land cover types in the southern part of the study area are desert steppe, semidesert, and barren areas; in the northern part, they are real steppe and forest. The main plants found in the region are *Achnatherum splendens, Populus euphratica*, Mongolia *Imperata cylindrica*, and other similar plants [27]. The region is a densely populated area of Mongolia, and the main occupations are animal husbandry and mining.

B. Data Sources

Thirty-two Landsat-8 operational land imager remote sensing images with 30-m resolution were selected from the United States Geological Survey website (http://earthexplorer.usgs.gov/). The imaging data were collected between June 2015 and October 2015, and the cloud coverage was less than 10%. The auxiliary data included the following:

1) vector map of the Mongolian administrative divisions in 2013 and vector data of the buffer zones within 200 km on both sides of the railway (source: Human-Earth thematic database of Chinese Academy of Sciences, http://www.data.ac.cn);
2) land cover data along the China–Mongolia railway (Mongolian section) in 2015 [28];
3) Google Earth online map;
4) field investigation data of desertification along the China–Mongolia railway.

C. Method

1) Correlation Analysis of Geographical Differentiation Law and Feature Space Modeling: Some studies have shown that feature spaces have clear biophysical significance [3], [19], [21]. In Albedo–NDVI and Albedo–MSAVI feature spaces, with an increase in desertification, the amount of surface vegetation gradually decreases, the NDVI and MSAVI correspondingly decrease, and the Albedo also increases accordingly [29], [30]. In Albedo–TGSI feature space, the more severe the desertification, the coarser the topsoil grain size composition, and the higher the value of TGSI [25]. Since different feature space models have certain limitations and corresponding applicable conditions [3], it is impossible to obtain accurate desertification information in large area with various geographical environment by relying on a single feature space model. Thus, this article attempts to build specific feature space models based on specific geographic regions in Mongolia.

According to the natural and cultural elements, such as the topography, climate, hydrology, and population resources for Mongolia, combined with the research results on the regionalization of livestock pasture in Mongolia [31], [32], Li *et al.* divided Mongolia into two major parts, the south and the north, by using the 200-mm equal-precipitation line of Mongolia as the dividing line between arid and semiarid areas [33]. Considering the influence of topography and river runoff on the local climate, the arid and semiarid areas in the north and south were further subdivided. In the southern part, the five provinces where the Altai mountains are located were classified as the Altai mountain region, and the remaining six provinces were classified as the Southern Gobi region. The northern part was divided into three parts by the Hentiy mountains and Orkhon river: The Northern forest region in the northwest, Central provinces and their northern region in the middle, and the Eastern Mongolian Plateau region in the east.

This study area mainly involves the Northern forest region, the Central provinces and their northern region, the Eastern Mongolian plateau region, and the Southern Gobi region. Combining the background data of land cover in Mongolia and vegetation cover data along the China–Mongolia railway, it can be observed that the distribution pattern along the railway is generally from northwest to southeast, from forest landscape to real steppe and desert steppe landscapes, and then to barren landscape. It has obvious zonal gradient law and the vegetation coverage gradually decreases from northwest to southeast. We found that the land cover type, vegetation coverage, and vegetation growth state of the Northern forest region were relatively close to that of the Central provinces and their northern region. They are both the areas with high vegetation coverage and a large forest ratio. Therefore, Hovsgol, Arhangay, Bulgan, and Orhon provinces in the Northern forest region are classified as the Central provinces and their northern region. The geographical partition layout along the China–Mongolia railway (Mongolian section) is shown in Fig. 2.

The Central provinces and their northern region has high vegetation cover. This region accounts for more than half of the country's population and has an average altitude of about 1500 m and a rainfall of about 300–400 mm [33]. The Eastern Mongolian Plateau region has relatively low vegetation cover. The average altitude is about 1000 m, and the annual precipitation is about 300–400 mm [33]. The Southern Gobi region has extremely low vegetation cover. The average altitude of this region is less than 1500 m, the terrain is relatively flat, and the annual precipitation in more than half of these areas is less than 100 mm [33].

In 2018, we finished the applicability analysis of three feature space models (Albedo–NDVI, Albedo–MSAVI, and Albedo–TGSI) by using Northwest Mongolia as an experimental area. We found that the Albedo–NDVI model was applicable to areas with high vegetation coverage and a large forest ratio, the Albedo–MSAVI model was applicable to areas with relatively low vegetation coverage, and the Albedo–TGSI model was

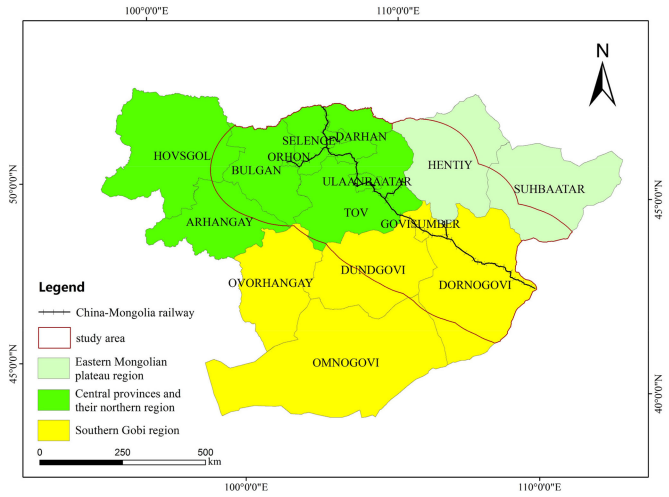

Fig. 2. Geographical zoning map of the study area.

applicable to areas with extremely low vegetation coverage and widespread distribution of Gobi Desert and barren land [3]. Accordingly, Albedo–NDVI, Albedo–MSAVI, and Albedo–TGSI were selected to extract desertification information for different regions, respectively.

2) Feature Space Construction of Desertification Information Extraction: Before the construction of feature spaces, the acquired images should be preprocessed for radiometric and atmospheric correction. Radiometric correction is the process of eliminating various distortions attached to the radiant brightness in the image data [34]. This article used radiometric correction modules via the ENVI 5.1 toolbox. Atmospheric correction is a process to eliminate radiation errors caused by atmospheric influences and invert the true surface reflectance of surface objects [35]. This article used the FLAASH module in ENVI 5.1 for atmospheric correction. Before this correction process, sensor type, ground elevation, image generation time, atmospheric model parameters, and other related information were input successively into this module. Remotely sensed images were cut and spliced with the vector boundary of Mongolian administrative divisions and areas within 200 km on both sides of the China–Mongolia railway. Finally, images covering the whole study area were synthesized.

NDVI, MSAVI, TGSI, Albedo, and other surface reference variables along the China–Mongolia railway (Mongolian section) were inversed based on the preprocessed remote sensing images.

The formula for NDVI is given as follows [36]:

$$\mathrm{NDVI} = (\mathrm{NIR} - \mathrm{RED})/(\mathrm{NIR} + \mathrm{RED}) \quad (1)$$

where NIR is the near-infrared band, and the RED is red band.

The formula for MSAVI is given as follows [20]:

$$\mathrm{MSAVI} = (2\mathrm{NIR} + 1 - \sqrt{(2\mathrm{NIR}+1)^2 - 8(\mathrm{NIR} - \mathrm{RED})})/2. \quad (2)$$

The formula for TGSI is given as follows [37]:

$$\mathrm{TGSI} = (\mathrm{RED} - \mathrm{BLUE})/(\mathrm{RED} + \mathrm{BLUE} + \mathrm{GREEN}) \quad (3)$$

where BLUE is the blue band and the GREEN is green band.

The formula for Albedo is given as follows [38]:

$$\mathrm{Albedo} = 0.356\mathrm{BLUE} + 0.13\mathrm{RED} + 0.373\mathrm{NIR} + 0.085\mathrm{SWIR1} + 0.072\mathrm{SWIR2} - 0.0018 \quad (4)$$

where SWIR1 and SWIR2 are the shortwave infrared bands.

To further reveal the interrelationships among multiple feature space variables, we randomly selected points along the railway. The first principle of the sample points selection was taking the study area as a whole and keeping the points evenly distributed. Due to the different spatial area of the three geographic zones, the number of sample points was also different for each zone. The greater the area, the greater the number of samples. Finally, 426, 606, and 837 points were selected using the ROI Tools of ENVI 5.1 in the Central provinces and their northern region, the Eastern Mongolian Plateau region, and the Southern Gobi region, respectively, and the corresponding Albedo, NDVI, MSAVI, and TGSI point values were extracted in turn by using the generated point files. Then, SPSS software was used to conduct statistical regression analysis of Albedo and corresponding NDVI, MSAVI, and TGSI in each geographical division. Finally, Albedo–NDVI, Albedo–MSAVI, and Albedo–TGSI feature space models were constructed for the three different geographic zones based on the obtained quantitative relations.

3) Desertification Information Extraction: According to the study of Verstraete and Pinty in 1996, different desertification lands can be effectively separated by dividing the Albedo–NDVI feature space in the vertical direction into changing trends of desertification [39]. The location of the vertical direction in Albedo–NDVI feature space can be well fitted by a simple binary linear polynomial expression. The result of the binary linear polynomial is the desertification difference index (DDI). That is, the DDI is an index that can be used to evaluate the degree of desertification in different regions through a fitting calculation of multiple bands. We used this method to divide Albedo–MSAVI and Albedo–TGSI feature space. Then, the corresponding DDI was obtained by fitting the vertical directions of the two feature spaces, respectively. The formulas are given as follows:

$$\mathrm{DDI}_{\mathrm{MAX}} = K_{\mathrm{MAX}} * \mathrm{NDVI} - \mathrm{Albedo} \quad (5)$$

$$\mathrm{DDI}_{\mathrm{MID}} = K_{\mathrm{MID}} * \mathrm{MSAVI} - \mathrm{Albedo} \quad (6)$$

$$\mathrm{DDI}_{\mathrm{MIN}} = K_{\mathrm{MIN}} * \mathrm{TGSI} + \mathrm{Albedo} \quad (7)$$

where $\mathrm{DDI}_{\mathrm{MAX}}$ is the desertification index of the Albedo–NDVI feature space model of the Central provinces and their northern region, $\mathrm{DDI}_{\mathrm{MID}}$ is the desertification classification index of the Albedo–MSAVI feature space model of the Eastern Mongolian Plateau region, and $\mathrm{DDI}_{\mathrm{MIN}}$ is the desertification classification index of the Albedo–TGSI feature space model of the Southern Gobi region. Multiply K_{MAX}, K_{MID}, and K_{MIN} by the different slopes of the different fitted lines in Albedo–NDVI, Albedo–MSAVI, and Albedo–TGSI feature spaces are all equal

Fig. 3. Actual photograph of withered grassland in Dornogovi province, Mongolia, during the summer growing season (Date: July 2019).

to -1. They are determined by the slope of the line fitted in the corresponding feature space.

Based on the principle of statistics, we respectively divided $\mathrm{DDI}_{\mathrm{MAX}}$, $\mathrm{DDI}_{\mathrm{MID}}$, and $\mathrm{DDI}_{\mathrm{MIN}}$ into five grades by the natural break classification method. These five levels are severe desertification, high desertification, medium desertification, low desertification, and nondesertification. The higher the degree of desertification, the more the value of NDVI and MSAVI decreases, and Albedo increases relatively, which leads to the lower the value of $\mathrm{DDI}_{\mathrm{MAX}}$ and $\mathrm{DDI}_{\mathrm{MID}}$. And the higher the degree of desertification, the more the value of TGSI increases, and the higher the value of $\mathrm{DDI}_{\mathrm{MIN}}$. The natural break classification method sets its boundaries on the natural grouping inherent in the data, where the data values are relatively different [40]. Additionally, every classification of the case is calculated by automatically selecting the smallest variance value. This way, the differences within the classes are the smallest, the differences between classes are the largest, and the optimal classification results are obtained.

In order to obtain more accurate desertification data, it is necessary to separate some information of naturally formed sand from other desertification information in advance and to categorize it independently. Generally, sand has a high reflectivity in each band except the thermal infrared band. Therefore, when the reflectivity data of multiple bands are added, sand has the highest value compared with five different levels of desertification. Therefore, sand information was extracted before the desertification information extraction. First, the reflectance of BLUE, GREEN, RED, NIR, SWIR1, and SWIR2 bands was added. Then, the natural discontinuity method was used to divide them into six categories; the category with the highest value was sand.

During the field investigation along the China–Mongolia railway in Mongolia, we found a large number of withered grasslands distributed in some areas of Dornogovi province in the south of the study area (as shown in Fig. 3). According to the introduction of relevant researchers in Mongolia, when the temperature is appropriate and water is sufficient, the withered grassland can quickly turn green in a short time. Because withered grassland is also a kind of desertification, we classified it as an independent desertification type and separated it from other desertification information in advance.

Vegetation indexes were divided into green vegetation indexes and yellow vegetation indexes according to the physical ecology state of withering [41]. Yellow vegetation indexes are indicators of leaf withering and yellowing, which is used to measure the shape change of vegetation reflection spectrum [42]. normalized difference senescent vegetation index (NDSVI) uses the sensitivity of the shortwave infrared band to the moisture content of vegetation [43]. When vegetation becomes decayed and withered, the index value would increase with the decrease in vegetation moisture content. Therefore, the information extraction of withered grassland can be carried out based on NDSVI.

The formula for NDSVI is given as follows:

$$\mathrm{NDSVI} = (\mathrm{SWIR1} - \mathrm{RED})/(\mathrm{SWIR1} + \mathrm{RED}). \quad (8)$$

4) Precision Evaluation: To verify the accuracy of the desertification information extraction method supported by multisource feature spaces and geographical zoning modeling, 426 verification points were evenly and randomly selected along the railway in strip, and each point was verified independently. These points consisted of 74 points of field verification and 352 verification points extracted from high-resolution remote sensing images. We carried out field investigations along the China–Mongolia railway and collected data from a total of 74 field verification points, including land cover type, vegetation coverage, and surface temperature and moisture parameters. In addition, verification points of high-resolution remote sensing images were uniformly selected and interpreted based on Google Earth data and true color images of Landsat 8. Then, the confusion matrix was constructed, and the producer accuracy, user accuracy, and overall classification accuracy were calculated. Finally, the desertification information extraction results were compared and analyzed with the existing high-resolution land cover data in 2015 [28].

III. Results

A. Linear Relationships Between Feature Space Variables

The linear formula and correlation coefficient results of the four characteristic space variables are shown in Fig. 4(a)–(c). It can be observed that Albedo has significant negative correlation with NDVI and MSAVI, with fitting degrees of 0.6805 and 0.7015, respectively. Albedo and TGSI are positively correlated linearly, with a fitting degree of 0.6302.

B. Desertification Pattern Along the China–Mongolia Railway (Mongolian Section)

Table I shows the *K* values of different DDIs. Fig. 5 shows the histograms for $\mathrm{DDI}_{\mathrm{MAX}}$, $\mathrm{DDI}_{\mathrm{MID}}$, and $\mathrm{DDI}_{\mathrm{MID}}$ and the location of the break points for classification based on the natural break classification method. Table II shows the range of $\mathrm{DDI}_{\mathrm{MAX}}$, $\mathrm{DDI}_{\mathrm{MID}}$, and $\mathrm{DDI}_{\mathrm{MID}}$ values for different desertification levels.

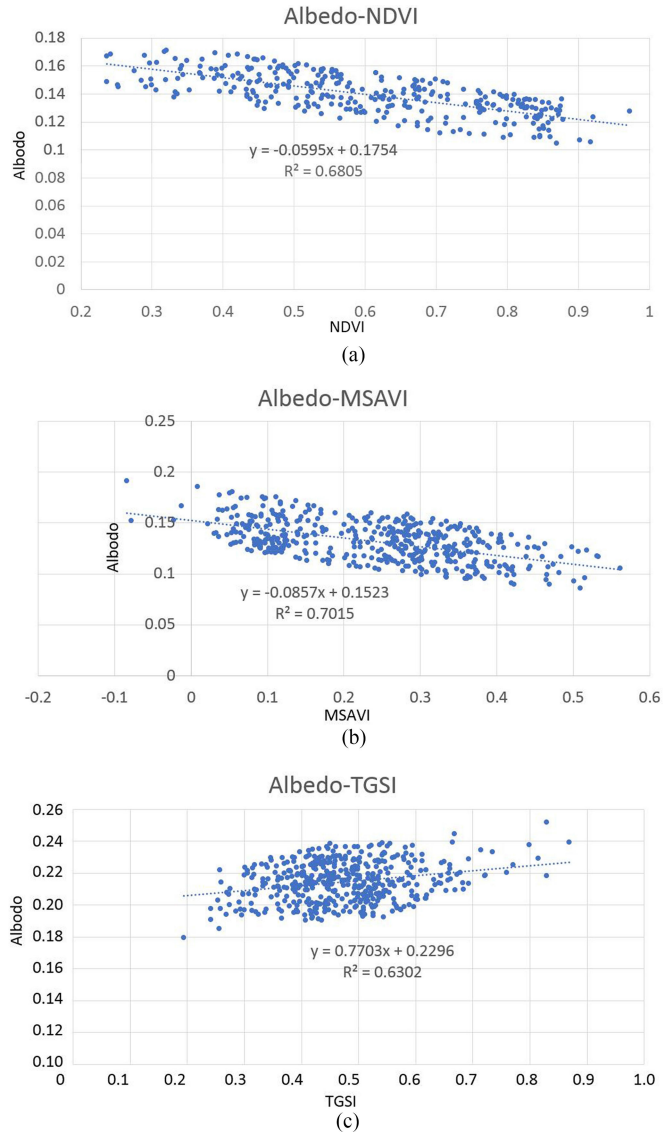

Fig. 4. Linear relationships between different feature space variables. (a). Albedo–NDVI. (b) Albedo–MSAVI. (c) Albedo–TGSI.

TABLE I
STATISTICAL TABLE OF *K* VALUES FOR THE THREE DESERTIFICATION DIFFERENT INDEXES

K	Value
K_{MAX}	16.81
K_{MID}	11.67
K_{MIN}	-1.30

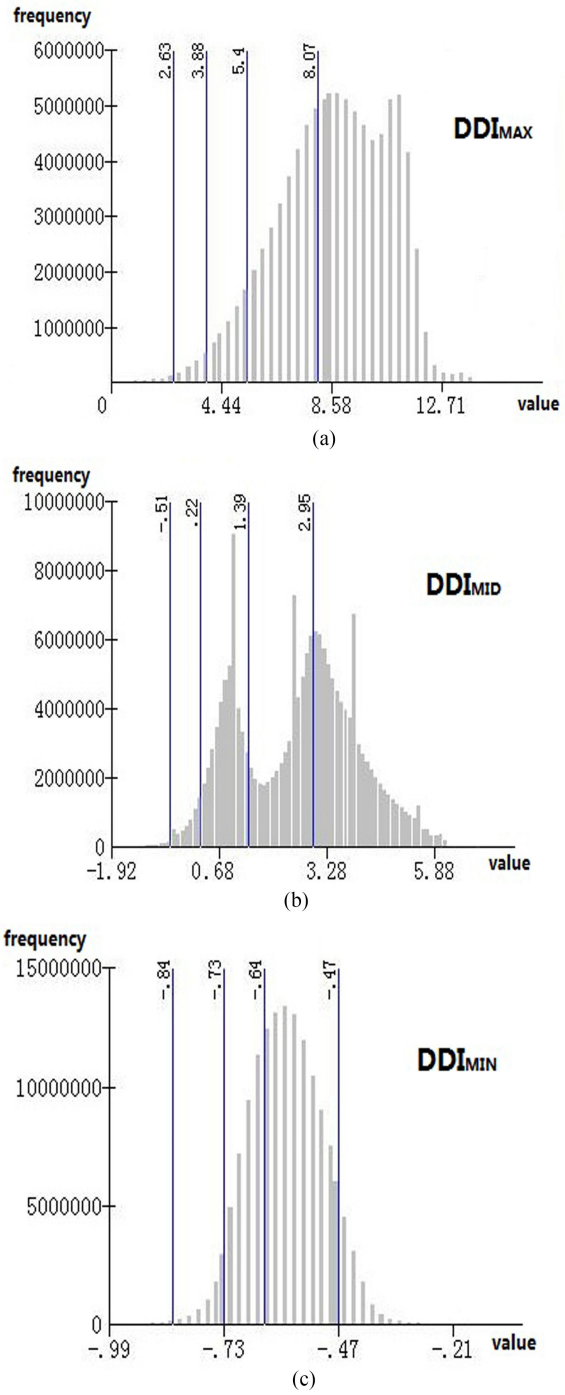

Fig. 5. Histograms of DDI values. (a) DDI_{MAX}. (b) DDI_{MID}. (c) DDI_{MIN}.

Then, we completed the extraction of desertification information and obtained the desertification data along the railway in 2015.

Fig. 6 shows the desertification distribution map along the China–Mongolia railway (Mongolian section) in 2015. Table III shows the desertification area and proportion. As shown in the figure, the nondesertification areas are mainly distributed in the northern part of the China–Mongolia railway in large blocks. It is specifically distributed in the east of Hovsgol, the northeast of Arhangay, most of Bulgan, Orhon, and Selenge, the east of Darhan, the northern and central parts of Tov, Ulaanbaatar, the northwest of Govisumber, and the north and west of Hentiy. The area of nondesertification regions is about 188 640.22 km^2, accounting for 45.32% of the total study area. Desertification areas are mainly distributed in the south, central, eastern, and northern regions along the railway. The area of desertification is about 223 049.34 km^2, accounting for 53.59% of the total study area. Among them, the withered grassland is mainly distributed

TABLE II
STATISTICAL TABLE OF THE RANGE OF DIFFERENT DDI VALUES FOR DIFFERENT DESERTIFICATION LEVELS

DDI	Level	Value Range
DDI_{MAX}	Non-desertification	> 8.07
	Low desertification	5.40 to 8.07
	Medium desertification	3.88 to 5.40
	High desertification	2.63 to 3.88
	Sever desertification	< 2.63
DDI_{MID}	Non-desertification	> 2.95
	Low desertification	1.39 to 2.95
	Medium desertification	0.22 to 1.39
	High desertification	-0.51 to 0.22
	Sever desertification	< -0.51
DDI_{MIN}	Non-desertification	< -0.84
	Low desertification	-0.84 to -0.73
	Medium desertification	-0.73 to -0.64
	High desertification	-0.64 to -0.47
	Sever desertification	> -0.47

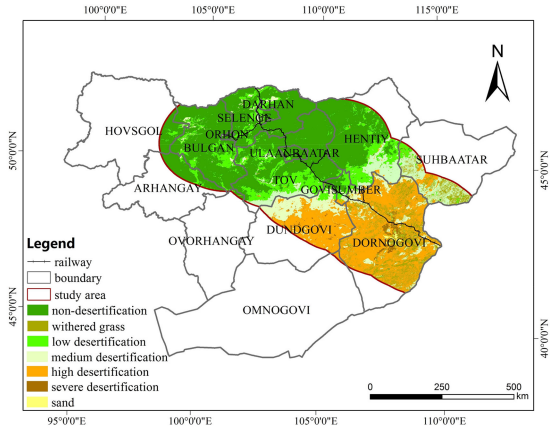

Fig. 6. Desertification distribution map along the China–Mongolia railway (Mongolian section) in 2015.

TABLE III
DESERTIFICATION AREAS AND THEIR PROPORTION ALONG THE CHINA–MONGOLIA RAILWAY (MONGOLIAN SECTION)

Level	Area (km^2)	Proportion (%)
Non-desertification	188,640.22	45.32
Withered grassland	21,322.74	5.12
Low desertification	50,013.64	12.02
Medium desertification	53,816.09	12.93
High desertification	92,112.81	22.13
Severe desertification	5784.06	1.39
Sand	4524.05	1.09
Total	416,213.61	100.00

in the Gobi region to the southeast of the railway in broken strip shapes. It is specifically distributed in the southwest of Suhbaatar and the east of Dornogovi, and a small number of explosive points are distributed in the western border area of Dornogovi. The area of withered grassland is about 21 322.74 km^2, accounting for 5.12% of the total study area. The low-desertification areas are mainly distributed in the northern and central parts along the railway. It is specifically distributed in the western border and the southeastern part of Bulgan, the north central part of Selenge, the western part of Darhan, the central and southern parts of Tov, the southwest and east of Hentiy, the northwest of Suhbaatar, and the northeast of Dundgovi. The area of low desertification is about 50 013.64 km^2, accounting for 12.02% of the total study area. The medium-desertification areas are mainly distributed in the central and eastern parts along the railway. It is specifically distributed in the southern border of Tov, the northern and central parts of Dundgovi, the southeastern part of Govisumber, the southeastern part of Hentiy, the southwestern part of Suhbaatar, and scattered areas in the northern and eastern parts of Dornogovi. The area of medium desertification is about 53 816.09 km^2, accounting for 12.93% of the total study area. The high-desertification areas are mainly distributed in the south of the railway. It is specifically distributed in the central and southern parts of Dundgovi, the south border area of Govisumber, the most of Dornogovi, and the southwest of Suhbaatar. The area of high desertification is about 92 112.81 km^2, accounting for 22.13% of the total study area. The severe desertification areas are mainly distributed in the central part of Dornogovi in strip shapes and sporadically distributed in the central part of Dundgovi in small blocks. The area of severe desertification is about 5784.06 km^2, accounting for 1.39% of the total study area. Sand is concentratively distributed in the central part of Dornogovi and sporadically in the central part of Dundgovi. Its distribution is concomitant with the areas of severe desertification. The area of sand is about 4524.05 km^2, accounting for 1.09% of the total study area.

TABLE IV
CONFUSION MATRIX OF THE DESERTIFICATION DATA

Level	Non	Withered grassland	Low	Medium	High	Sever	Sand
Non	96	0	0	3	0	0	0
Withered grassland	3	45	0	6	3	0	0
Low	9	3	51	3	0	0	0
Medium	6	3	3	42	3	0	0
High	0	3	0	0	63	3	3
Sever	0	0	3	0	3	42	3
Sand	0	0	0	0	0	0	24

C. Accuracy Assessment

Table IV shows the confusion matrix of the desertification data. Table V shows the producer accuracies and user accuracies of the desertification data. The results show that the overall classification accuracy of desertification data is about 85.21% for 2015. The Kappa coefficient is 0.8235. The producer accuracies of severe desertification, high desertification, medium desertification, low desertification, withered grassland, nondesertification, and sand are 93.33%, 87.50%, 77.78%, 89.47%, 83.33%, 84.21%, and 80.00%, respectively. The user accuracies of severe desertification, high desertification, medium desertification, low desertification, withered grassland, nondesertification, and sand are 82.35%, 87.50%, 73.68%, 77.27%, 78.95%, 96.97%, and 100.00%, respectively.

TABLE V
PRODUCER ACCURACY AND USER ACCURACY OF DESERTIFICATION DATA ALONG THE CHINA–MONGOLIA RAILWAY (MONGOLIA SECTION)

Level	Producer Accuracy (%)	User accuracy (%)
Non-desertification	84.21	96.97
Withered grassland	83.33	78.95
Low desertification	89.47	77.27
Medium desertification	77.78	73.68
High desertification	87.50	87.50
Sever desertification	93.33	82.35
Sand	80.00	100.00

IV. DISCUSSION

According to the desertification distribution pattern along the China–Mongolia railway (Mongolia section) for 2015, the desertification areas were concentrated in the central and southern parts of the region and sporadically in the northern areas. The desertification areas of different degrees have obvious transitional distribution, and the desertification degree gradually aggravates from northwest to southeast. According to the distribution map of land cover along the China–Mongolia railway in 2015 obtained by Wang *et al*. [28], it can be found that the vegetation coverage along the railway decreased gradually from northwest to southeast, and the landscape pattern also showed a transitional trend from forest to desert steppe and then to barren land. This is consistent with the characteristics and transitional trend of desertification distribution along the railway obtained in this article.

Some scholars tried to extract desertification information by interpreting land cover types. That is to say, from the perspective of landscape pattern, desert steppe and barren land are classified as desertification land types. Although the land cover type map and desertification status map are not of the same type, desertification inevitably causes the changes in land cover types and produces special land cover types. Therefore, the current desertification condition can be indirectly reflected by land cover type map to a certain extent. The desertification data obtained in this article were compared with the land cover data along the railway from Wang *et al*. for 2015 [28]. The results showed that the area of desertification land obtained by remote sensing image interpretation accounted for 46.68% of the total area, which was lower than the desertification rate of 53.59% obtained in this article. Because land cover monitoring is insensitive to some weak information in arid and semiarid areas, it is easy to underestimate the desertification land cover. Compared with land cover mapping, the desertification information extraction method constructed in this article can depict detailed desertification information.

The results were also compared with the desertification distribution data released by the Mongolia government in 2017 [2], which showed that the general desertification rate of Mongolia was 76.8%. In this article, the research area is approximately distributed longitudinally in central Mongolia. Almost half of the study area is in the north with widespread forests and grasslands, and another half of the study area is in the south with Gobi Desert spread wide. Therefore, the real desertification rate of this region should be lower than the general desertification rate in Mongolia (76.80%). Because of the land cover characteristics mentioned above, we can infer that about half of the land should suffer from desertification of different degrees in this study area, and thus it is very close to our result of 53.59%.

During the field investigations along the China–Mongolia railway (Mongolian section), we found a large amount of withered grassland distributed in some parts of the Gobi area. Because of the high temperature and low precipitation, most of the vegetation in Gobi cannot survive, and a large number of grasslands were in a withered and yellowing state. However, with global warming, the temperature during April and September in Gobi is conducive to vegetation growth. If the precipitation during this season is relatively sufficient and concentrated, the withered grassland can quickly turn green in a short time. The desertification distribution map shows that the withered grassland is mainly distributed in the southeastern region along the railway. This may be associated with the East Asian monsoon from the Pacific Ocean. It brings relatively appropriate precipitation to the eastern and southeastern regions of Mongolia. Furthermore, the monsoon makes it possible for the withered grassland in the above-mentioned areas to turn green and ensures that withered grassland can always stay in the yellow state in summer, rather than completely withering and dying. The leaf color of withered grassland is yellow, the chlorophyll content is very low, and the water content is low. This is why the commonly used greenness vegetation index (such as NDVI and MSAVI) and Albedo are difficult to effectively extract. Due to its similarity with barren land in water content and greenness, most studies on desertification information extraction unilaterally misclassified it as high-desertification areas. United Nations Convention to Combat Desertification Combating Desertification defines "desertification" as land degradation in arid, semiarid, and dry subhumid areas, caused by factors that include climate change and human activities [44]. Under the influence of global warming, large areas of green vegetation in Gobi dry up and turn yellow in summer and further degenerate into withered grassland. Therefore, the withered grassland can be classified as desertification land. The withered grassland has the possibility of turning green and regeneration, and even if it does not turn green, it is still significantly different from barren land and other levels of desertification land. Therefore, it should be classified as a new and separate type of desertification land in Mongolia. Thus, this article proposed a desertification classification system that included six levels, i.e., severe desertification, high desertification, medium desertification, low desertification, withered grassland, and nondesertification. The accuracy of desertification classification could be increased by effectively extracting withered grassland information.

The region along the China–Mongolia railway (Mongolia section) is located in arid and semiarid areas. Desertification information is easily confused with other weak vegetation cover information. Previous studies have shown that with an increase in desertification, the surface conditions obviously change, the amount of surface vegetation gradually decrease, the NDVI and MSAVI correspondingly decrease, and the Albedo also increases

accordingly [29], [30]. The more severe the desertification, the rougher the topsoil grain size composition, and the higher the value of TGSI [25]. This means that these surface reference variables have clear biophysical significance and can reflect changes in desertification. By constructing feature spaces, we can make full use of multidimensional remote sensing information, enhance the sensitivity of desertification information, and improve the accuracy of desertification information extraction. We obtained the DDI by linear fitting of the vertical position in the feature spaces. By constructing the DDI, we realized the transformation from the surface reference variables with biophysical meanings into remote sensing spectral information. Thus, we realized the quantitative calculation and automatic classification of desertification information. However, relying on a single feature space model can only obtain relatively high-precision desertification information extraction results in specific local areas with single geographical environment. If only the Albedo–NDVI feature space model is used to extract desertification information from the areas along the railway, more accurate results can be obtained for the areas with high vegetation coverage. However, NDVI cannot be well expressed in areas with sparse vegetation because it is influenced by the soil background (such as the central and eastern parts of the study area), thus reducing the classification accuracy of the medium-desertification areas. This is especially true in the south of the study area, since this area is mainly barren land and the vegetation coverage is very low. Thus, it is no longer suitable to use the vegetation growth status as the criterion for judging high and severe desertification. If NDVI continues to be used as one of the criteria for the degree of desertification, it will inevitably reduce the classification accuracy of the medium-, high-, and severe-desertification areas. If only the Albedo–MSAVI feature space model is selected, high-accuracy results can be obtained in the areas with relatively low vegetation coverage, like the central and eastern parts of the study area. However, no matter how much we improve the sensitivity of the vegetation index, the classification accuracy of high and severe desertification areas will not greatly improve in the southern part of the study area and areas with extremely low vegetation coverage. So, it is necessary to extract the desertification information from the surface soil texture and granularity in these areas. Therefore, TGSI can be used as one of the indicators for desertification assessment, thereby improving the classification accuracy of areas with high desertification level. However, if the Albedo–TGSI feature space model is used in the northern, central, and eastern parts of the study area with high or relatively high vegetation coverage area, there will be a lack of vegetation biomass interpretation. Consequently, the influence of vegetation factors on desertification information extraction will be ignored, thus reducing the classification accuracy of the areas with relatively low desertification level. To sum up, we found that the selection of a single feature space model cannot complete the high-precision and refined desertification information extraction. Only by combining the results of geographical zoning and making full use of the applicability of various feature space models, building the desertification fine inversion method based on multisource feature space, and geographical zoning modeling, we can effectively extract the weak desertification information, and obtain the desertification information with high precision in complex geographical environment and large areas.

Compared with previous studies on desertification information extraction, this article selected data sources with higher resolution, introduced a variety of surface reference variables to construct the corresponding composite feature space model, and improved the accuracy of desertification information extraction. At present, desertification monitoring studies in the China–Mongolia–Russia economic corridor are mostly conducted using large-scale desertification information extraction with MODIS data with a spatial resolution of 1 km. Moreover, the data products are relatively old, mostly concentrated in the early 21st century and the 1990s, and there have been few new data after 2010 [13]–[15]. These findings generally assess the spatiotemporal characteristics and changing trends of desertification at a macroscale, but do not easily reveal detailed status, and cannot provide direct and accurate data support for desertification control and regional risk prevention. At the same time, studies on desertification information extraction based on 30-m resolution or feature space models have only been carried out in a small area and cannot be extended to expand to a larger geographical area [19] [24] [45]. Therefore, this article used Landsat 8 images with a resolution of 30 m as the basic data and constructed feature space model suitable for each geographic partition based on geographic differentiation rules to greatly enhance the description of detailed information and improve the accuracy. At present, there are still some problems with this article that require further improvement. We only used the "natural break classification method" to classify DDI without expert experiment support. In the future, we will adopt human–computer interaction to classify DDI, so as to improve accuracy in some sensitive and transitional areas. In addition, currently a few feature space variables were introduced, including NDVI, MSAVI, TGSI, and Albedo. More reference variables like land productivity could be involved in the further study.

V. Conclusion

Aiming at the scientific problem of accurately extracting desertification information being difficult in the region along the China–Mongolia railway, we first proposed a method for fine extracting desertification information in large areas and complex geographical environment. Based on the multisource geographical data, the region along the China–Mongolia railway (Mongolian section) was divided into three geographical parts. According to the vegetation coverage characteristics and the applicability of various feature space models to different geographical regions, Albedo–NDVI, Albedo–MSAVI, and Albedo–TGSI feature space models were, respectively, constructed for the Central provinces and their northern region, the Eastern Mongolian Plateau region, and the Southern Gobi region, we first obtained the desertification data with a resolution of 30 m in this region, analyzed the mechanism of the method and why withered grassland was classified as a separate

type of desertification, and compared with previous studies on desertification information extraction. This article proved that it is feasible to finely extract desertification information in complex geographical environment and large areas supported by multisource feature spaces and geographical partition modeling. We found that the DDI calculated by fitting the vertical direction of the feature spaces can be used to realize the transformation from the surface reference variables with biophysical meanings into remote sensing spectral information and complete the quantitative calculation and automatic classification of desertification information. Faced with new challenges in the classification and extraction of desertification in the Mongolian Plateau under the influence of global warming and monsoons, we established and improved a desertification classification system that included six levels (severe desertification, high desertification, medium desertification, low desertification, withered grassland, and non-desertification), and enhanced the accuracy of desertification classification. This article could provide a refined inversion method and data product support for ecological risk control of desertification in larger arid and semiarid areas.

ACKNOWLEDGMENT

The authors would like to thank the members of the research teams of the Institute of Geographic Sciences and Natural Resources Research, Chinese Academy of Sciences, and the National University of Mongolia for their support in field work and the discussion section. The authors would also like to thank the editor of this journal and the anonymous reviewers during the revision process.

REFERENCES

[1] S. Eckert, F. Hüsler, H. Liniger, and E. Hodel, "Trend analysis of MODIS NDVI time series for detecting land degradation and regeneration in Mongolia," *J. Arid Environ*., vol. 113, no. 2, pp. 16–28, Feb. 1959.

[2] Y. I. Chen and H. Chang, "Nearly 80% of land in Mongolia suffers from desertification in different degrees." 2017. [Online]. Available: http://world.people.com.cn/n1/2017/0617/c1002-29345905.html

[3] H. S. Wei *et al.*, "Desertification information extraction based on feature space combinations on the Mongolian plateau," *Remote Sens.*, vol. 10, no. 10, Oct. 2018, Art. no. 1614.

[4] J. Guli, X. Chen, and A. M. Bao, "Coverage extraction and up-scaling of sparse desert vegetation in arid area," *Chinese J. Appl. Ecology*, vol. 20, no. 12, pp. 2925–2934, Dec. 2009.

[5] A. M. Holm, S. W. Cridland, and M. L. Roderick, "The use of time-integrated NOAA NDVI data and rainfall to assess landscape degradation in the arid shrubland of Western Australia," *Remote Sens. Environ.*, vol. 85, pp. 145–158, May 2003.

[6] R. Geerken and M Ilaiwi, "Assessment of rangeland degradation and development of a strategy for rehabilitation," *Remote Sens. Environ.*, vol. 90, pp. 490–504, Apr. 2004.

[7] K. J. Wessels, F. V. Bergh, and R. J. Scholes, "Limits to detectability of land degradation by trend analysis of vegetation index data," *Remote Sens. Environ.*, vol. 125, pp. 10–22, Oct. 2012.

[8] R. G. Kremer and S. W. Running, "Community type differentiation using NOAA /AVHRR data within a sagebrush-steppe ecosystem," *Remote Sens. Environ.*, vol. 46, pp. 311–318, Dec. 1993.

[9] X. H. Yang and L. J. Ci, "Progress on remote sensing-based desertification assessment," *World Forestry Res.*, vol. 19, no. 6, pp. 11–17, 2006.

[10] X. T. Li, J. Bai, G. L. Li, G. P. Luo, J. Guli, and J. L. Li, "Comparison of methods based on MODIS for estimating sparse vegetation fraction across desert in Xinjiang," *Arid Land Geography*, vol. 36, no. 3, pp. 502–511, May 2013.

[11] F. Basso, E. Bove, S. Dumontet, A. Ferrara, M. Pisante, and G. Quaranta, "Evaluating environmental sensitivity at the basin scale through the use of geographic information systems and remotely sensed data: An example covering the Agri basin (southern Italy)," *Catena*, vol. 40, pp. 19–35, Jun. 2000.

[12] K. Rasmussen, B. Fog, and J. E. Madsen, "Desertification in reverse observations from northern Burkina Faso," *Global Environ. Change*, vol. 11, pp. 271–282, Dec. 2001.

[13] A. X. Liu, C. Y. Wang, J. Wang, and X. M. Shao, "Method for remote sensing monitoring of desertification based on MODIS and NOAA/AVHRR data," *Trans. Chin. Soc. Agric. Eng.*, vol. 23, pp. 145–150, Oct. 2007.

[14] B. Unurbaatar and Y. H. Caoligeer, "The spatial and temporal changes of desertification in the Mongolian plateau from 2000–2010," in *Proc. Risk Anal. Crisis Response Inf. Technol.—China Disaster Prevention Assoc. Risk Anal. Professional Committee Annu. Meeting*, Beijing, China, pp. 637–643, Mar. 1–2, 2014.

[15] Y. Zhuo, "The ration remote sensing method study of desertification of mongolia plateau based on MODIS data," Master's thesis, Inner Mongolia Normal Univ., Hohhot, China, 2007.

[16] Y. Y. Li, X. C. Yang, X. H. Zhu, and B. Xu, "The application of remote sensing technology to land desertification monitoring," *Prog. Geography*, vol. 28, no. 1, pp. 55–62, Jan. 2009.

[17] E. K. Albalawi and L. Kumar, "Using remote sensing technology to detect, model and map desertification: A review," *J. Food, Agric. Environ.*, vol. 11, pp. 791–797, 2013.

[18] Q. Guo, B. Fu, P. Shi, T. Cudahy, J. Zhang, and H. Xu, "Satellite monitoring the spatial-temporal dynamics of desertification in response to climate change and human activities across the Ordos Plateau, China," *Remote Sens*., vol. 9, May 2017, Art. no. 525.

[19] Y. N. Zeng, N. P. Xiang, Z. D. Feng, and H. Hu, "Albedo-NDVI space and remote sensing synthesis index models for desertification monitoring," *Sci. Geogr. Sin.*, vol. 26, pp. 75–81, Jan. 2006.

[20] J. Qi, A. Chehbouni, A. R. Huete, Y. H. Kerr, and S. Sorooshian, "A modified soil adjusted vegetation index," *Remote Sens. Environ.*, vol. 48, pp. 119–126, May 2015.

[21] J. Feng, J. L. Ding, and W. Y. Wei, "Research on soil salinization in Weikui Oasis based on the characteristic space of Albedo-MSAVI," *J. China Rural Water Hydropower*, vol. 2, pp. 147–152, 2018.

[22] Z. D. Zhu and T. Wang, "An analysis on the trend of land dessertification in northern China during the last decade based on examples from some typical areas," *Acta Geographica Sin.*, vol. 57, no. 4, pp. 430–440, 1990.

[23] Q. Liu, G. Liu, and C. Huang, "Monitoring desertification processes in Mongolian Plateau using MODIS tasseled cap transformation and TGSI time series," *J. Arid Land*, vol. 10, no. 1, pp. 12–26, Feb. 2018.

[24] M. Lamchin *et al.*, "Assessment of land cover change and desertification using remote sensing technology in a local region of Mongolia," *Adv. Space Res.*, vol. 57, no. 1, pp. 64–77, Jan. 2016.

[25] M. Lamchin *et al.*, "Correlation between desertification and environmental variables using remote sensing techniques in Hogno Khaan, Mongolia," *Sustainability*, vol. 9, Apr. 2017, Art. no. 581.

[26] Y. J. Wei, L. Zhen, X. L. Liu, and B. Ochirbat, "Land use change and its driving factors in Mongolia from 1992 to 2005," *Chin. J. Appl. Ecol.*, vol. 19, pp. 1995–2002, Oct. 2018.

[27] X. X. Yue, "Study on the flora of seed plants in the Mongolian plateau," Ph.D. thesis, Inner Mongolia Agric. Univ., Hohhot, China, 2011.

[28] J. L. Wang *et al.*, "Spatio-temporal pattern of land degradation along the China-Mongolia railway (Mongolia)," *Sustainability*, vol. 11, no. 9, May 2019, Art. no. 2705.

[29] S. G. Li, Y. Harazono, T. Oikawa, H. L. Zhao, Z. Y. He, and X. L. Chang, "Grassland desertification by grazing and the resulting micrometeorological changes in inner Mongolia," *Agric. Forest Meteorol.*, vol. 102, pp. 125–137, May 2000.

[30] Y. Wang, and X. Yan, "Climate change induced by southern hemisphere desertification," *Phys. Chem. Earth*, vol. 102, pp. 40–47, Dec. 2017.

[31] Q. S. Yang, L. S. Gao, and X. M. Li, *Mongolian Geography*, Changchun, China: Northeast Normal Univ. Press, 1994, pp. 17–32.

[32] F. Q. Wang, *Sustainable Development of Mongolia Grassland Animal Husbandry*. Huhhot, China: Inner Mongolia Univ., 2010.

[33] Y. F. Li, J. L. Wang, and J. X. Zhu, "Landscape pattern analysis of Mongolia based on the geographical partitions," *Arid Land Geography*, vol. 39, no. 4, pp. 817–827, Apr. 2016.

[34] S. Zhu and Y. Chen, "Methods for atmospheric radiation correction," *J. Geospat. Inf.*, vol. 8, no. 1, pp. 119–122, 2010.

[35] W. Zheng and Z. Y. Zeng, "A review on methods of atmospheric correction for remote sensing images," *Remote Sens. Inf.*, vol. 4, pp. 66–70, Apr. 2004.
[36] T. N. Carlson and D. A. Ripley, "On the relation between NDVI, fractional vegetation cover, and leaf area index," *Remote Sens. Environ.*, vol. 62, pp. 241–252, Dec. 1997.
[37] J. Xiao, Y. Shen, R. Tateishi, and W. Bayaer, "Development of topsoil grain size index for monitoring desertification in arid land using remote sensing," *Int. J. Remote Sens.*, vol. 27, pp. 2411–2422, Jun. 2006.
[38] S. Liang *et al.*, "Narrowband to broadband conversions of land surface albedo: II. Validation," *Remote Sens. Environ.*, vol. 84, pp. 25–41, Jan. 2003.
[39] M. M. Verstraete, and B. Pinty, "Designing optimal spectral indexes for remote sensing applications," *Remote Sens. Environ.*, vol. 34, pp. 1254–1265, Sep. 1996.
[40] W. U. Zeng-Hai and L. I. Tao, "The comprehensive performance evaluation of the high-tech development zone: Analysis based on the natural breakpoint method," *Statist. Inf. Forum*, vol. 3, pp. 82–88, Mar. 2013.
[41] W. M. Ren, "Study on the applicability of vegetation index to calculate regional vegetation coverage," Master thesis, Northwest Univ., Xian, China, 2012.
[42] W. N. Lei and Z. M. Wen, "Extraction of structured vegetation cover index for Loess Area in North Shaanxi based on TM images," *Chin. J. Appl. Ecol.*, vol. 20, no. 11, pp. 2736–2742, Nov. 2009.
[43] R. C. Marsett *et al.*, "Remote sensing for grassland management in the arid southwest," *Rangeland Ecol. Manage.*, vol. 59, pp. 530–540, Sep. 2006.
[44] L. H. Ci, "Understanding on the term of "Desertification"," *Chin. Sci. Technol. Terms J.*, vol. 2, no. 4, pp. 11–13, 2000.
[45] Z. Ma, Y. Xie, J. Jiao, and X. Wang, "The construction and application of an Aledo–NDVI based desertification monitoring model," *Procedia Environ. Sci.*, vol. 10, pp. 2029–2035, Dec. 2011.

Haishuo Wei was born in Laiwu, China, in 1994. He received the B.Sc. degree in surveying and mapping in 2017 from the Shandong University of Technology, Zibo, China, where he is currently working toward the M.S. degree in remote sensing.

His research interests include desertification information extraction and land degradation monitoring.

Juanle Wang was born in Luoyang, China, in 1976. He received the B.Sc. degree in surveying engineering and the M.S. degree in geodesy and survey engineering from the China University of Mining and Technology, Xuzhou, China, in 1998 and 2002, respectively; and the Ph.D. degree in cartography and geography information system from the Institute of Geographic Sciences and Natural Resources Research, Chinese Academy of Sciences, Beijing, China, in 2005.

He is currently a Professor with the Institute of Geographic Sciences and Natural Resources Research, Chinese Academy of Sciences. His research interests include land use changes, land degradation monitoring, and the sharing of resource and environmental science data.

Baomin Han was born in Linshu, China, in 1969. He received the Ph.D. degree in geodesy and survey engineering from the Institute of Geodesy and Geophysics, Chinese Academy of Sciences, Wuhan, China, in 2003.

He is currently a Professor with the Shandong University of Technology. His research interests include land use changes, desertification, and GPS precise positioning.